

Improved aggregation-induced emission behavior in D- π -A architectures by modifying the donor units

Jing-Yi Cao,^a Guang Yang,^a Zeng-Min Xue,^a Wen-Xuan Zhao,^a Shu-Hai Chen,^{a,*} Hong-Tao Lin,^a Takehiko Yamato,^{b,*} Carl Redshaw,^c Dan-Yu Gu,^d Chuan-Zeng Wang^{a,*}

- ^a School of Chemistry and Chemical Engineering, Shandong University of Technology, Zibo 255049, P. R. China.
- ^b Department of Applied Chemistry, Faculty of Science and Engineering, Saga University Honjo-machi 1, Saga 840-8502 Japan.
- ^c Chemistry, School of Natural Sciences, The University of Hull, Cottingham Road, Hull, Yorkshire HU6 7RX, UK.
- ^d Instrumentation and Service Center for Molecular Sciences, Westlake University, Hangzhou 310024, Zhejiang Province, China.

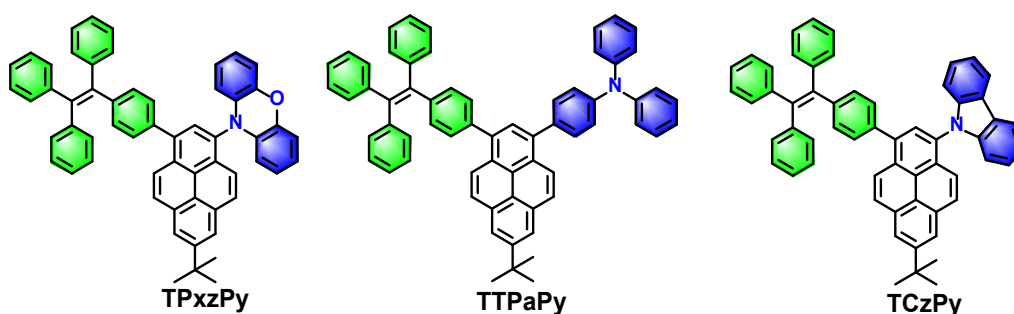
Abstract: With the development of aggregation-induced emission (AIE) in optoelectronic devices, stimulus-responsive sensors, optical storage and bioimaging, the design and synthesis of efficient AIE luminogens remains a challenge. Herein, a series of asymmetric pyrene derivatives were prepared by stepwise functionalization at the 1-, 3-positions using traditional reactions. The experimental results show that a promising white-light emitting material (Commission Internationale de L'Eclairage (CIE): $x = 0.32, y = 0.31$), namely **TPxzPy**, which has completely separated the highest occupied molecular orbital (HOMOs) and lowest unoccupied molecular orbital (LUMOs) distribution, was produced. Moreover, a new strategy was established to construct pyrene-based AIE luminogens along the short axis. All compounds exhibited higher emission efficiency in the solid or aggregated state *versus* in solution, especially for **TTPaPy** with a competitive photoluminescence quantum yield as high as 76.2%. The present work provides a feasible strategy to construct pyrene-based AIE materials for optoelectronic devices.

Introduction

In recent years, the development of efficient luminescent materials has attracted more and more attention, especially for practical applications and academic research. In particular, organic solid luminescent materials have promising applications in optoelectronic devices, anti-counterfeiting technology and fluorescent sensors.¹⁻³ However, the application and development of luminescent materials has been somewhat limited due to the aggregation caused quenching (ACQ) effect in the solid state or films and even in concentrated solution.⁴⁻⁵ In 2001, the relationship between AIE phenomenon and the working mechanisms of restriction of intramolecular motion (RIM), restriction of intramolecular rotation (RIR) and restriction of intramolecular vibration (RIV) were established by Tang and other workers.⁶⁻¹² This work helped to greatly broaden the research and application field of organic luminescent materials.

Pyrene is a typical polycyclic aromatic hydrocarbon (PAHs) compound, and its planar configuration with extended sp^2 -hybridized carbon scaffolds and ten easily modified active sites have inspired a large number of researchers and has made pyrene the core of choice in fundamental and applied photoelectric material research.¹³⁻¹⁵ However, the ACQ effect impacts on the emission efficiency in pyrene-based systems when they are aggregated or clustered.¹⁶ Much effort has been devoted to inhibiting the ACQ behavior in pyrene-based photoelectric materials, and an effective approach was established by employing either bulky pendant groups or propeller-shaped frameworks.¹⁷⁻²⁰ By benefiting from the presence of AIE luminogens (AIEgens), a more efficient strategy that has received more attention involves the introduction of an AIE unit to construct a twisted fragment based on the RIR mechanism.^{21,22} In view of the difference in activity of the ten peripheral reactive positions at the pyrene core,²³ other synthetic work has focused on regio-selectivity and purification. Typically, the 1-, 3-, 6-, and 8-positions²⁴, 2-, 7-positions²⁵, 4-, 5-, 9-, and 10-positions,^{26,27} 1-, 3-, 5-, or 9-positions²⁸ are preferred given their respective chemical equivalence. In stark contrast, asymmetrical substitution at the above-mentioned positions is rather challenging due to steric and isomerization effects. However, the excellent photoelectric properties of asymmetrically substituted pyrene derivatives have encouraged researchers to persevere with such efforts.²⁹⁻³¹

In the present work, a new series of tetraphenylethylene-fused asymmetrically 1,3-disubstituted pyrene molecules have been designed based on our previous synthetic strategy.^{32,33} In particular, three tunable donor- π -acceptor (D- π -A) type pyrene-based AIEgens were afforded by introducing different electron-donating groups at the 3-position of the pyrene core along the short axis (Scheme 1). All the luminogens exhibit significant solvatochromism and high photoluminescence efficiency in the solid state. Thus, an efficient strategy to improve and tune the emission behavior has been established with the aid of the AIE unit and intramolecular charge-transfer (ICT) theory.



Scheme 1. Chemical structures of the luminogens TPxzPy, TTPaPy and TCzPy.

Experimental Section

All reagents were purchased from commercial suppliers (Leyan reagent, Aladdin) and were used without further purification. All the reactions were carried out using a round bottom flask under a nitrogen or argon atmosphere in anhydrous solvents. ¹H and ¹³C NMR spectra were recorded in CDCl₃ on a WJGS-037 Bruker AVANCE III 400 MHz NMR spectrometer, using tetramethyl silane (TMS) as the internal standard. Mass spectra were recorded on an Agilent 1290 Infinity. UV-vis absorbance and photoluminescence (PL) spectra were recorded on a Shimadzu UV-3600 and a Fluorescence spectrophotometer F-380A, respectively. Photoluminescence quantum efficiencies (PLQYs) were measured using a Quantaaurus-QY C11347-11.

Synthesis of 7-*tert*-butyl-1-(4-(1,2,2-triphenylvinyl)phenyl)pyrene

A mixture of 7-*tert*-butyl-1-bromopyrene (168.63 mg, 0.5 mmol), 1-(4-phenylboronic acid pinacol ester)-1,2,2-triphenylethene (240.66 mg, 0.525 mmol) in toluene (15 mL) and ethanol (4 mL) at room temperature were stirred under argon, and a 2 M aqueous

solution of K_2CO_3 (20 mL) and Pd (PPh_3)₄ (28.89 mg, 0.025 mmol) was added. After the mixture was stirred for 30 min. at room temperature under argon, the mixture was heated to 90°C for 24 h with stirring. After cooling to room temperature, the mixture was quenched with water, extracted with CH_2Cl_2 (2 × 30 mL), washed with water and brine. The organic extracts were dried with $MgSO_4$ and evaporated. The residue was purified by column chromatography eluting with CH_2Cl_2 /hexane (1 : 4) to afford a white solid in 42% yield. M.P. 218–220°C; ¹H NMR (400 MHz, $CDCl_3$): (δ= ppm): δ_H = 8.22 (s, 1H, pyrene-H), 8.19 (s, 1H, pyrene-H), 8.15 (d, *J* = 8.0 Hz, 1H, pyrene-H), 8.08 (d, *J* = 9.2 Hz, 3H, pyrene-H), 8.05 (s, 2H, pyrene-H), 7.99 (d, *J* = 9.2 Hz, 1H, pyrene-H), 7.91 (d, *J* = 8 Hz, 1H, pyrene-H), 7.37 (d, *J* = 8.4 Hz, 2H, Ph-H), 7.23–7.08 (m, 17H, Ph-H), 1.58 (s, 9H, *t*Bu); ¹³C NMR (100 MHz, $CDCl_3$): δ_C = 149.1, 143.8, 143.7, 143.6, 142.6, 141.3, 140.7, 139.2, 137.3, 131.5, 131.4, 131.3, 131.2, 130.8, 130.3, 129.9, 128.2, 127.74, 127.72, 127.6, 127.5, 127.3, 127.1, 126.54, 126.52, 126.4, 125.1, 124.9, 124.4, 123.1, 122.3, 121.9, 35.2, 31.9. FAB-MS: *m/z* calcd for C₄₆H₃₆ 588.2817 [M⁺]; found 588.2808 [M⁺].

Synthesis of 7-*tert*-butyl-1-(4-(1,2,2-triphenylvinyl)phenyl)-3-bromopyrene

7-*tert*-Butyl-1-(4-(1,2,2-triphenylvinyl)phenyl)pyrene (294.4 mg, 0.5 mmol) and BTMABr₃ (292.46 mg, 0.75 mmol) were added to a solution of CH_2Cl_2 (5 mL) and MeOH (12mL). The resulting mixture was stirred at 26 °C for 16 h under a nitrogen atmosphere. The mixture was evaporated to dryness and taken up with CH_2Cl_2 . The organic layer was washed with H₂O, dried over $MgSO_4$, filtered and evaporated to dryness. Recrystallization afforded 310 mg of an orange solid in 92.8% yield. M.P. 250–252°C; ¹H NMR (400 MHz, $CDCl_3$): (δ= ppm): δ_H = 8.40 (d, *J* = 9.2 Hz, 1H, pyrene-H), 8.25 (s, 1H, pyrene-H), 8.22 (s, 1H, pyrene-H), 8.17–8.13 (t, *J* = 9.2 Hz, 2H, pyrene-H), 8.01 (d, *J* = 2.8 Hz, 2H, pyrene-H), 7.34 (d, *J* = 8.4 Hz, 2H, Ph-H), 7.22–7.09 (m, 17H, Ph-H), 1.58 (s, 9H, *t*Bu). FAB-MS: *m/z* calcd for C₄₆H₃₅Br 666.1922 [M⁺]; found 666.1914 [M⁺].

Synthesis of 7-*tert*-butyl-1-(4-(1,2,2-triphenylvinyl)phenyl)-3-(10*H*-phenoxazin-10-yl)pyrene (TPxzPy)

A mixture of 7-*tert*-butyl-1-(4-(1,2,2-triphenylvinyl)phenyl)-3-bromopyrene (166.92 mg, 0.25 mmol), phenoxazine (68.7 mg, 0.375 mmol) and NaOtBu (72.1, 0.75 mmol) in toluene (10 mL) at room temperature was stirred under argon, and a 0.025 M aqueous solution of P(*t*Bu)₃ (0.025 mL) and Pd₂(dba)₃ (11.45 mg, 0.0125 mmol) was added. After the mixture was stirred for 30 min. at room temperature under argon, the mixture was heated to 110°C for 24 h with stirring. After cooling to room temperature, the mixture was quenched with water, extracted with CH₂Cl₂ (2 × 30 mL), washed with water and brine. The organic extracts were dried with MgSO₄ and evaporated. The residue was purified by column chromatography eluting with CH₂Cl₂ /hexane (1 : 5) to give TPxzPy (110 mg) as a yellow solid in 57.3% yield. M.P. >300°C; ¹H NMR (400 MHz, DMSO-*d*₆): (δ = ppm): δ_H = 8.46 (d, *J* = 8.0 Hz, 2H, pyrene-*H*), 8.33–8.25 (m, 2H, pyrene-*H*), 8.14–8.07 (m, 2H, pyrene-*H*), 7.96 (s, 1H, pyrene-*H*), 7.49 (d, *J* = 8.0 Hz, 2H, Ph-*H*), 7.26–7.03 (m, 17H, Ph-*H*), 6.83 (d, *J* = 8.0 Hz, 2H, phenoxazine-*H*), 6.70–6.66 (t, *J* = 8 Hz, 2H, phenoxazine-*H*), 6.54–6.50 (t, *J* = 8.4 Hz, 2H, phenoxazine-*H*), 5.67 (d, *J* = 8.0 Hz, 2H, phenoxazine-*H*), 1.56 (s, 9H, *t*Bu); ¹³C NMR (100 MHz, CDCl₃): (δ = ppm): δ_C = 149.9, 143.8, 143.78, 143.74, 143.2, 141.5, 140.6, 139.7, 138.1, 131.53, 131.51, 131.49, 131.43, 131.3, 130.8, 129.9, 129.2, 128.7, 128.5, 127.9, 127.8, 127.7, 126.8, 126.7, 126.6, 126.5, 124.9, 123.5, 123.33, 123.30, 122.9, 122.3, 113.7, 35.3, 31.9. FAB-MS: *m/z* calcd for C₅₈H₄₃NO 769.3345 [M⁺]; found 769.3335 [M⁺].

Synthesis of 7-*tert*-butyl-1-tetra(4-(1,2,2-triphenylvinyl)phenyl)-3-(4-diethylaminophenyl)pyrene (TTPaPy)

A mixture of 7-*tert*-butyl-1-(4-(1,2,2-triphenylvinyl)phenyl)-3-bromopyrene (233.69 mg, 0.35 mmol), 4-(diphenylamino) phenylboronic acid and pinacol ester (194.93 mg, 0.525 mmol) in toluene (12 mL) and ethanol (3 mL) at room temperature was stirred under argon, and a 2 M aqueous solution of K₂CO₃ (14 mL) and Pd (PPh₃)₄ (20.22 mg, 0.0175 mmol) was added. After the mixture was stirred for 30 min. at room temperature

under argon, it was heated to 90°C for 24 h with stirring. After cooling to room temperature, the mixture was quenched with water, extracted with CH₂Cl₂ (2 × 30 mL), washed with water and brine. The organic extracts were dried with MgSO₄ and evaporated. The residue was purified by column chromatography eluting with CH₂Cl₂/hexane (1 : 5) to give **TTPaPy** as a yellow solid in 74.8% yield. M.P.285–287°C; ¹H NMR (400 MHz, CDCl₃): (δ = ppm): δ_H = 8.27 (d, *J* = 9.2 Hz, 1H, pyrene-*H*), 8.19 (s, 2H, pyrene-*H*), 8.09 (d, *J* = 9.2 Hz, 1H, pyrene-*H*), 8.03–7.98 (t, *J* = 9.2, 2H, pyrene-*H*), 7.92 (s, 1H, pyrene-*H*), 7.53 (d, *J* = 8.4 Hz, 2H, Ph-*H*), 7.40 (d, *J* = 8.0 Hz, 2H, Ph-*H*), 7.34–7.29 (t, *J* = 8.4 Hz, 4H, Ph-*H*), 7.24–7.06 (m, 25H, Ph-*H*), 1.59 (s, 9H, *t*Bu); ¹³C NMR (100 MHz, CDCl₃): δ_C = 149.2, 147.8, 147.1, 143.9, 143.86, 143.81, 142.7, 141.4, 140.8, 139.1, 137.0, 136.8, 135.1, 131.5, 131.47, 131.45, 131.3, 131.2, 130.0, 129.4, 128.9, 127.83, 127.81, 127.7, 127.6, 127.55, 127.50, 127.4, 126.6, 126.59, 126.55, 125.50, 125.3, 125.2, 124.6, 123.5, 123.4, 123.1, 122.2, 35.3, 32.0. FAB-MS: *m/z* calcd for C₆₄H₄₉N 831.3865 [M⁺]; found 831.3856 [M⁺].

Synthesis of 7-*tert*-butyl-1-(4-(1,2,2-triphenylvinyl)phenyl)-3-(9*H*-carbazol-9-yl)pyrene (TCzPy)

A mixture of 7-*tert*-butyl-1-(4-(1,2,2-triphenylvinyl)phenyl)-3-bromopyrene (233.69 mg, 0.35 mmol), carbazole (87.79 mg, 0.525 mmol) and NaO*t*Bu (100.91mg, 1.05 mmol) in toluene (15 mL) at room temperature was stirred under argon, and a 0.035 M aqueous solution of P(*t*Bu)₃ (0.035 mL) and Pd₂(dba)₃ (16.03 mg, 0.0175 mmol) was added. After the mixture was stirred for 30 min. at room temperature under argon, the mixture was heated to 110°C for 24 h with stirring. After cooling to room temperature, the mixture was quenched with water, extracted with CH₂Cl₂ (2 × 30 mL), washed with water and brine. The organic extracts were dried with MgSO₄ and evaporated. The residue was purified by column chromatography eluting with CH₂Cl₂/hexane (1 : 4) to give **TCzPy** (85.6 mg) as a white solid in 32.4% yield. M.P.260–262°C; ¹H NMR (400 MHz, CDCl₃): (δ = ppm): δ_H = 8.28–8.22 (m, 5H, pyrene-*H*), 8.12 (d, *J* = 9.6 Hz, 1H, pyrene-*H*), 8.02 (s, 1H, pyrene-*H*), 7.92 (d, *J* = 9.2 Hz, 1H, Ph-*H*), 7.55 (d, *J* = 9.2 Hz, 1H, Ph-*H*), 7.42 (d, *J* = 8.4 Hz, 2H, Ph-*H*), 7.36–7.32 (m, 4H, Ph-*H*), 7.21–7.07 (m,

19H, Ph-*H*), 1.59 (s, 9H, *t*Bu); ^{13}C NMR (100MHz, CDCl_3): δ_{C} =149.9, 143.7, 143.69, 143.62, 143.1, 142.4, 141.5, 140.6, 138.2, 138.14, 138.11, 135.3, 131.5, 131.4, 131.2, 130.9, 130.5, 129.9, 128.8, 128.7, 128.6, 128.4, 127.8, 127.7, 127.5, 126.7, 126.59, 126.55, 126.3, 126.0, 125.0, 123.4, 123.19, 123.15, 122.9, 122.5, 120.4, 119.9, 110.34, 84.4, 31.9, 24.9. FAB-MS: m/z calcd for $\text{C}_{58}\text{H}_{43}\text{N}$ 753.3396 [M^+]; found 753.3386 [M^+].

Results and Discussion

Synthesis and characterization

The synthetic procedures for the three luminogens **TPxzPy**, **TTPaPy** and **TCzPy** and their precursors are outlined in the experimental section and in [Scheme S1](#). A stepwise functionalized strategy was performed by a Suzuki–Miyaura cross-coupling reaction and a Buchwald–Hartwig amination reaction starting from two brominated intermediates, respectively. Characterization data including ^1H and ^{13}C NMR spectroscopy, and high-resolution mass spectrometry, and related results are given in the [Supporting Information \(Figs. S1–S14, ESI†\)](#). Excellent solubility in common organic solvents was observed for the three compounds, which will be beneficial for applications in photoelectric materials.

Photophysical properties

The UV-vis absorption and emission properties of luminogens **TPxzPy**, **TTPaPy** and **TCzPy** were studied in dilute solution and in the solid state; the parameters are listed in [Table 1](#). As shown in [Fig. 1A](#), the three luminogens present two sets of absorption bands including a high-energy band centered at 280–295 nm and a broad absorption band with a low-energy absorption centered at 335–360 nm. The high-energy absorption is mainly assigned to the locally excited (LE) state of the pyrene core, and slight differences for the maximum absorption wavelength was observed at 287 nm for **TPxzPy**, 291 nm for **TTPaPy**, 284 nm for **TCzPy**, which is attributed to the substituent effect.³⁴ Comparatively speaking, the low-energy absorption band is relatively more sensitive and affected than the high-energy band by the nature of the substituent at the 3-position of the pyrene core. The low-energy absorption band was mainly attributed

to the ICT transition along the short axis from the 3-position to the 1-position through the π -conjugated pyrene core.³⁵ There is an obvious red-shift from **TCzPy** (325 nm) to **TTPaPy** (342 nm) and **TPxzPy** (352 nm), and this result further verifies the adjustability of the CT transition.

Table 1. The photophysical properties of **TPxzPy**, **TTPaPy** and **TCzPy**.

Comp.	λ_{abs} (nm) sol ^[a]	λ_{em} (nm) sol ^[b] /solid	$\Phi_{\text{FL}}^{\text{[c]}}$ (%) sol ^[b] /solid	HOMO ^[d] (eV)	LUMO ^[d] (eV)	$\Delta E_{\text{g}}^{\text{[d]}}$ (eV)	$\alpha_{\text{AIE}}^{\text{[e]}}$	τ (ns)
TPxzPy	287, 352	409, 567/509	2.7 / 17.6	-4.59	-1.77	2.82	5.9	35.03
TTPaPy	291, 342	473 / 476	7.4 / 76.2	-4.84	-1.57	3.27	10.1	2.69
TCzPy	284, 325	414 / 460	0.2 / 27.5	-5.17	-1.75	3.42	9.5	7.57

^a 1×10^{-5} M in THF, λ_{abs} is the absorption band appearing at the longest wavelength.

^b 1×10^{-6} M in THF, λ_{em} is the fluorescence band appearing at the shortest wavelength.

^c Absolute quantum yield (± 0.01 – 0.03).

^d B3LYP/6-31G* using Gaussian.

^e α_{AIE} is the AIE factor defined by the following equation: $\alpha_{\text{AIE}} = I_{\text{THF/water (0:9.9, v/v)}}/I_{\text{THF}}$.

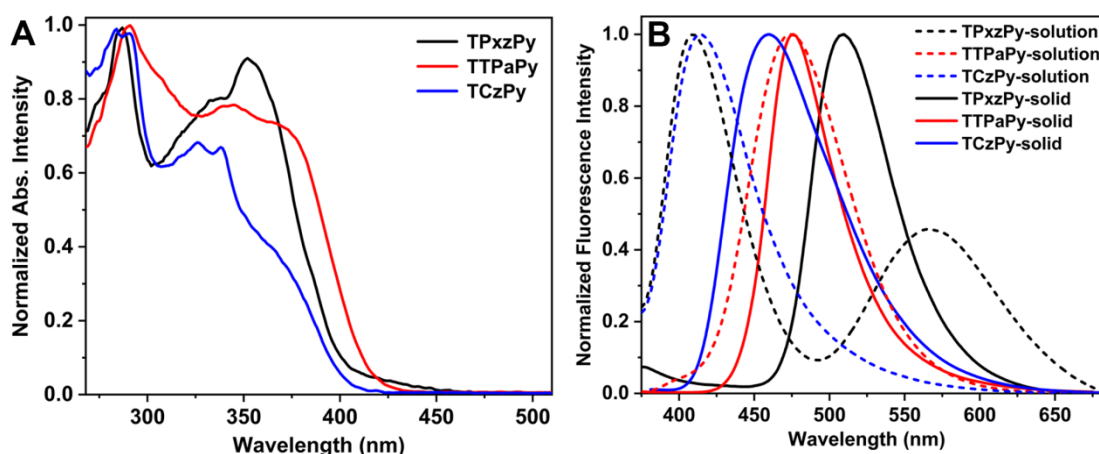


Fig. 1. UV-vis absorption (A) and emission spectra (B) for the luminogens **TPxzPy**, **TTPaPy** and **TCzPy** in THF solution and in the solid state, respectively.

Then, the emission behavior of three luminogens **TPxzPy**, **TTPaPy** and **TCzPy** were recorded in diluted THF solution and in the solid state. As shown in **Fig. 1B**, the three compounds exhibited distinct emission properties in dilute THF solution. Interestingly, **TPxzPy** shows a dual emission while the other two luminogens revealed a single emission color, which is attributed to the conformational isomerization of phenoxazine in the ground state.³⁶ Moreover, further evidence supports the above conclusion for the absorption behavior, with varying degrees of intramolecular charge-

transfer in this system resulting in significant emission wavelength shifts of more than 150 nm ($\lambda_{\max \text{ em}} = 409$ nm and 567 nm for **TPxzPy**, 473 nm for **TTPaPy** and 414 nm for **TCzPy**). Specifically, the low emission wavelengths at 409 nm for **TPxzPy** and 414 nm for **TCzPy** are attributed to the monomeric emission of the pyrene unit, while the ICT emission state plays a dominant role in the long emission wavelength at 567 nm for **TPxzPy**. To further interpret the emission mechanism, a study of the solvatochromic effect was carried out in different organic solvents of various polarities (cyclohexane, 1,4-dioxane, tetrahydrofuran (THF), dichloromethane (DCM) and dimethylformamide (DMF)). The solvatochromic effects for all compounds basically support our interpretation of the ICT effect.³⁷ As shown in Fig. 2 and Figs. S15–S16 (ESI[†]), the value of the red-shift of the maximum emission peak on increasing the polarity follows the order **TPxzPy** > **TTPaPy** > **TCzPy**. It is exciting that a single molecular organic near white-light-emitting compound was achieved with the CIE coordinate of $x = 0.32$, $y = 0.31$; the visual results are presented in Fig. 2B as an inset.

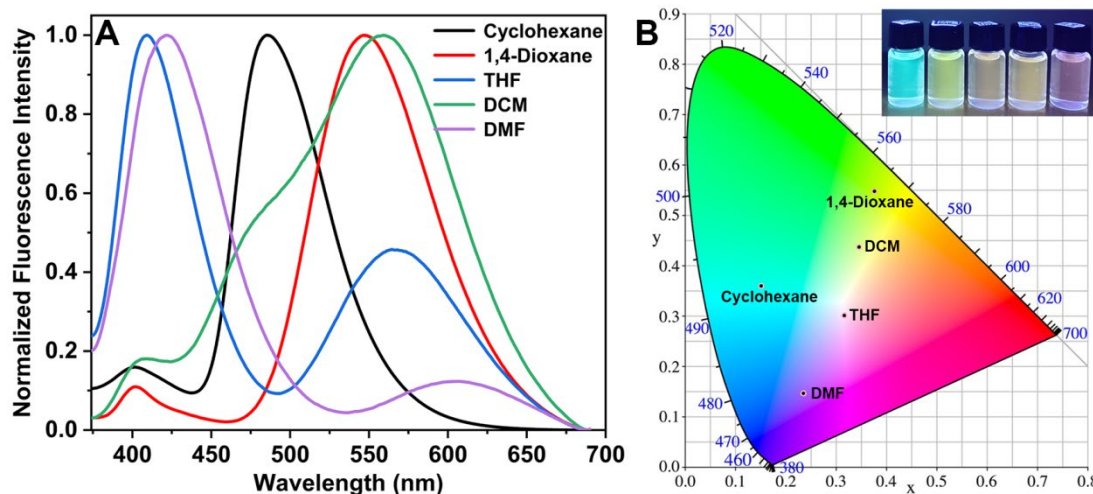


Fig. 2. (A) Solvatochromism effect of emission spectra for **TPxzPy** in different organic solvents with various polarities; (B) The CIE 1931 chromaticity diagram for **TPxzPy**. (Inset: Fluorescent photographs of **TPxzPy** in cyclohexane, 1,4-dioxane, THF, DCM and DMF, respectively).

Subsequently, the emission properties were recorded in the solid state. A consistent emission wavelength shift is present compared to the diluted solution ($\lambda_{\max \text{ em}} = 509$ nm for **TPxzPy**, 476 nm for **TTPaPy** and 460 nm for **TCzPy**). All compounds revealed various degrees of red-shift compared to their emission behavior in dilute organic solution, which is likely the result of the differences in the molecular aggregates.²⁹ The

fluorescence lifetimes of the three luminogens were measured to evaluate their electronic transition in the excitation state (see Figs. S17–S19, ESI†); the value of lifetimes (τ) are in the range 2.69–35.03 ns in the solid state. A long fluorescence lifetime, especially for **TPxzPy**, makes it a promising candidate for organic electronic devices.³⁸

The fluorescence quantum yields (Φ_{FL}) were recorded in diluted solution and the solid state. As expected, these luminogens exhibit higher value of Φ_{FL} in the solid state (17.6% for **TPxzPy**, 76.2% for **TTPaPy**, 27.5% for **TCzPy**) than in solution (2.7% for **TPxzPy**, 7.4% for **TTPaPy**, 0.2% for **TCzPy**). The radiative decay pathways are further triggered by restricting the intramolecular rotations with the aid of highly twisted conformations.³⁹

AIE properties

The AIE properties of the luminogens **TPxzPy**, **TTPaPy** and **TCzPy** were investigated systematically in THF/H₂O mixtures, and the spectra are described in Figs. 3 and S20–S23, ESI†. Different from traditional pyrene derivatives, the above mentioned luminogens present obvious AIE properties with high emission intensity in the aggregated state. Taking **TPxzPy** as an example, two sets of emission peaks were observed in the short-wave region centered at 395–420 nm and in the long-wave region with a range of 500–590 nm. As shown in Fig. 3A, upon increasing the water fraction (f_w), the emission intensity is obviously enhanced. In the long-wave region, the PL intensity of luminogen **TPxzPy** displayed a slight weakening and red-shift from 566 nm to 584 nm upon increasing f_w from 0% to 60%, which is largely due to the ICT emission and increased solvent polarity. When the f_w in the solvent mixture increased to 99%, the emission intensity rapidly rises by 6-fold with a larger blue-shift from 584 nm to 514 nm due to molecular aggregation (see Figs. 3B and S20 ESI†).⁴⁰ On the other hand, in the short-wave region, the emission intensity gradually decreased upon increasing f_w , which results from the weakened monomeric emission in the aggregated state.³⁴ Overall, **TPxzPy** is an AIE-active material with an α_{AIE} value of 5.9. Similarly, luminogen **TTPaPy** exhibited typical AIE characteristics with a higher α_{AIE} value

(10.1), a red-shift from 464 nm to 490 nm and blue-shift from 490 nm to 458 nm with the turning point $f_w = 60\%$ (see Fig. S20 and S22 ESI†). As depicted in Fig. 4, a persistent red-shift of maximum emission wavelength and emission enhancement approximately 10-fold ($\alpha_{AIE} = 9.5$) occurred during the process of increasing f_w from 0% to 99%, which is largely due to RIR. These attractive results provide a facile and efficient strategy to design more significant molecules for practical applications.

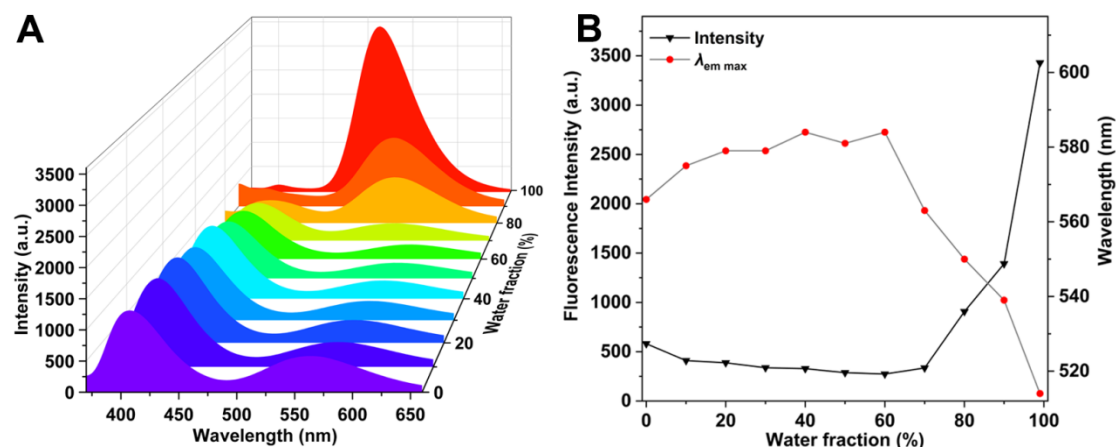


Fig. 3. (A) The fluorescence spectra of TPxzPy in mixed H₂O/THF solutions (1×10^{-6} M); (B) Plots of maximum emission wavelength and emission intensity for the long-wave region at different fractions (0–99 vol%) for TPxzPy.

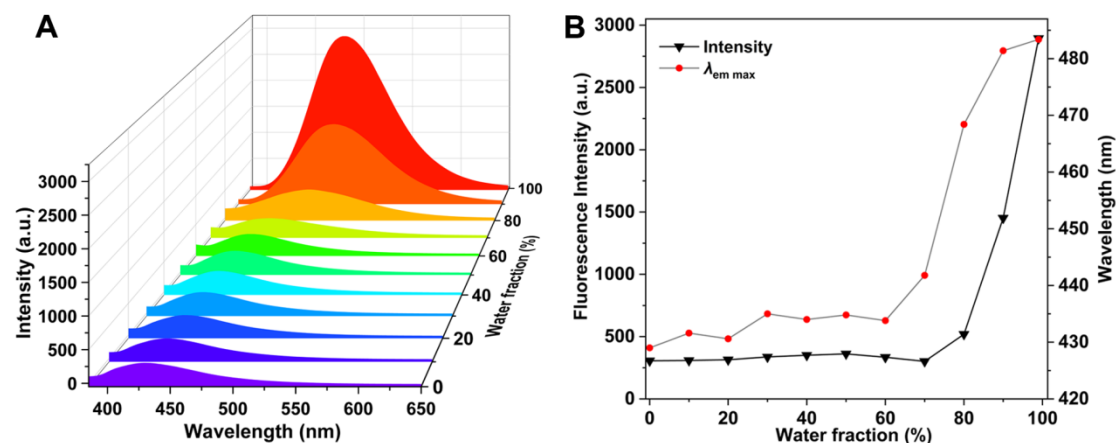


Fig. 4. (A) The fluorescence spectra of TCzPy in mixed H₂O/THF solutions (1×10^{-6} M); (B) Plots of maximum emission wavelength and emission intensity at different fractions (0–99 vol%) for TCzPy.

Theoretical calculations

Furthermore, density functional theory (DFT) calculations were performed to evaluate the influence of the D- π -A architectures and electron delocalization on the optical

properties at the B3LYP/6-31G* level.^{41,42} The distributions and energy levels of their HOMO and LUMO are presented in Fig. 5. For the AIEgens **TPxzPy**, **TTPaPy** and **TCzPy**, similar distributions of LUMOs were observed, and the LUMOs are primarily localized on the pyrene core and a portion of the TPE unit. In sharp contrast, the distributions of HOMOs displayed significant differences in these asymmetrically 1,3-disubstituted pyrene-based AIEgen systems. The HOMO of **TCzPy** is almost completely localized over the entire molecule, while the HOMO is mainly distributed at the pyrene core and triphenylamine unit. Most dramatically, a completely separated HOMO and LUMO distribution for the AIEgen **TPxzPy** was present, and the HOMO is just spread over the phenoxazine unit. As expected, distinct energy gaps (ΔE_g) confirmed our previous interpretation of ICT behavior in this type of AIEgens. Moreover, it is an interesting result that the completely separated HOMOs and LUMOs, particularly for **TPxzPy**, are important for efficient luminescent materials in certain circumstances, which could facilitate the synthesis of thermally activated delayed fluorescence (TADF) emitters by adjusting the energy gap.⁴³ Both theoretical and experimental results show that this type of molecule exhibits competitive photophysical properties compare to similar pyrene-based luminogens or AIEgens, in terms of luminescence efficiency, potential application of white-light emitting material with dual emission bands, and tunability of optoelectronic properties.

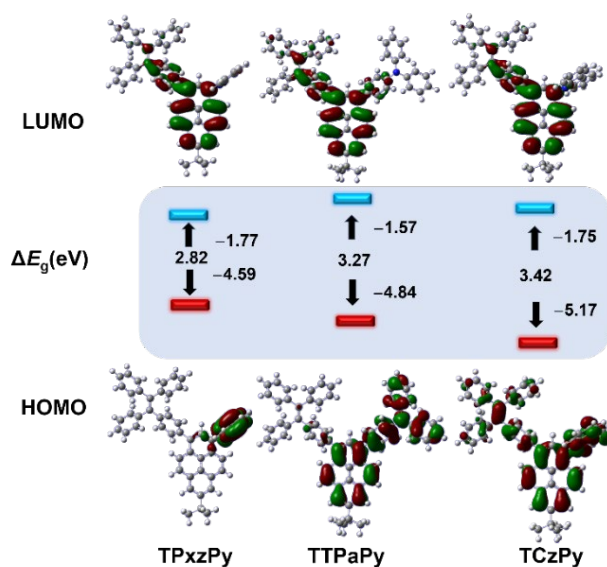


Fig. 5. Frontier-molecular-orbital distributions and energy level diagrams for **TPxzPy**, **TTPaPy** and

TCzPy by DFT calculations.

Conclusions

In summary, three asymmetrically 1,3-disubstituted pyrene-based AIEgens with different electron-donating groups were prepared in reasonable yield. These AIEgens exhibited tuneable emission properties both in dilute solution and in the solid state. Even in related structural systems, distinct optical properties were clearly present because of the different electron-donating groups at the 3-position of the pyrene core. TPxzPy displayed a dual emission with near-white-light fluorescence in organic solution, and is a rare example of a single molecular white-light emitting material. In addition, excellent emission efficiency in the solid state or films as AIE-active molecule makes these promising optoelectronic materials. This work provides an efficient strategy to construct pyrene-based AIEgens along the short axis based on ICT effects.

Conflicts of interest

The authors declare that they have no known competing financial interests or personal relationships that could have appeared to influence the work reported in this paper.

Acknowledgements

This work was performed under the Cooperative Research Program of “Network Joint Research Center for Materials and Devices (Institute for Materials Chemistry and Engineering, Kyushu University)”. We would like to thank the Natural Science Foundation of Shandong Province (Grant No. ZR2019BB067), this research used resources of the Advanced Light Source, which is a DOE Office of Science User Facility under contract no. DE-AC02-05CH11231. CR thanks the University of Hull for support.

References

- [1] Tomas SW, Joly GD, Swager TM. Chemical Sensors Based on Amplifying Fluorescent Conjugated Polymers. *Chem. Rev.* 2007;107:1339–1386.

- [2] Ma SQ, Du SJ, Pan GC, Dai ST, Xu B, Tian WJ. Organic molecular aggregates: From aggregation structure to emission property. *Aggregate* 2021;2:e96.
- [3] Hang J, Sun N, Chen P, Tang R, Li Q, Ma D, Li Z. Largely blue-shifted emission through minor structural modifications: molecular design, synthesis, aggregation induced emission and deep-blue OLED application. *Chem. Commun.* 2014;50:2136–2138.
- [4] Hong Y, Lam JWY., Tang BZ, Aggregation-induced emission. *Chem. Soc. Rev.* 2011;40:5361–5388.
- [5] Mei J, Leung NLC, Kwok RTK, Lam JWY, Tang BZ. Aggregation-induced emission: together we shine, united we soar. *Chem. Rev.* 2015;115:11718–11940.
- [6] Luo J, Xie Z, Lam JWY, Cheng L, Chen H, Qiu C, Kwok HS, Zhan X, Liu Y, Zhu D, Tang BZ. Aggregation-induced emission of 1-methyl-1,2,3,4,5-pentaphenylsilole. *Chem. Commun.* 2001;1740–1741.
- [7] Peng Q, Shuai ZG. Molecular mechanism of aggregation-induced emission. *Aggregate* 2021;2:e91.
- [8] Li J, Wang J, Li H, Song N, Wang D, Tang BZ. Supramolecular materials based on AIE luminogens (AIEgens): construction and applications. *Chem. Soc. Rev.* 2020;49:1144–1172.
- [9] Mao D, Liu B. Biology-oriented design strategies of AIE theranostic probes. *Matter* 2021; 4:350–376.
- [10] Li ZY, Zeng XY, Gao CM, Song JZ, He F, He T, Guo H, Yin J. Photoswitchable diarylethenes: From molecular structures to biological applications. *Coordination Chemistry Reviews* 2023; 497:215451.
- [11] Li ZY, Chen S, Huang YR, Zhou H, Yang SR, Zhang HN, Wang MX, Guo H, Yin J. Photoswitchable AIE photosensitizer for reversible control of singlet oxygen generation in specific bacterial discrimination and photocontrolled photodynamic killing of bacteria. *Chemical Engineering Journal* 2022;450:138087.
- [12] Zhang HN, He CJ, Shen LM, Tao WJ, Zhu JH, Song JZ, Li ZY, Yin J. Membrane-targeting amphiphilic AIE photosensitizer for broad-spectrum bacteria imaging and photodynamic killing of bacteria. *Chinese Chemical Letters* 2023;34:108160.
- [13] Figueira-Duarte TM and Müllen K. Pyrene-Based Materials for Organic Electronics. *Chem. Rev.* 2011;111:7260–7314.

- [14] Feng X, Hu JY, Redshaw C and Yamato T. Functionalization of Pyrene To Prepare Luminescent Materials—Typical Examples of Synthetic Methodology. *Chem. – Eur. J.* 2016; 22:11898–11916.
- [15] Amouri H. Luminescent Complexes of Platinum, Iridium, and Coinage Metals Containing N-Heterocyclic Carbene Ligands: Design, Structural Diversity, and Photophysical Properties. *Chem. Rev.* 2023;123:230–270.
- [16] Förster T, Kasper K and Bunsenges B. Ein Konzentrationsumschlag der Fluoreszenz des Pyrens. *Phys. Chem.* 1955;59: 976–978.
- [17] Islam MM, Hu Z, Wang QS, Redshaw C, Feng X. Pyrene-based aggregation-induced emission luminogens and their applications. *Mater. Chem. Front.* 2019;3:762–781.
- [18] Oh JW, Lee YO, Kim TH, Ko KC, Lee JY, Kim H, Kim JS. Enhancement of Electrogenerated Chemiluminescence and Radical Stability by Peripheral Multidonors on Alkynylpyrene Derivatives. *Angew. Chem. Int. Ed.* 2009;48:522–2524.
- [19] Wang CZ, Feng X, Kowser Z, Wu C, Ather T, Elsegood RJ, Redshaw C, Yamato T. Pyrene-based color-tunable dipolar molecules: Synthesis, characterization and optical properties, *Dyes and Pigments* 2018;153:125–131.
- [20] Li HL, Cao JY, Yu ZD, Yang G, Xue ZM, Wang CZ, Zhao WX, Zhao Y, Redshaw C, Yamato T. A substituent-dependent deep-blue pyrene-based chemosensor for trace nitroaniline sensing. *Mater. Chem. Front.* 2023;7:3365–3372.
- [21] Zhao ZJ, Chen SM, Lam JWY, Lu P, Zhong YC, Wong KS, Kwok HS, Tang BZ. Creation of highly efficient solid emitter by decorating pyrene core with AIE-active tetraphenylethene peripheries. *Chem. Commun.* 2010;46:2221–2223.
- [22] Zeng J, Qiu NL, Zhang JY, Wang XH, Redshaw C, Feng X, Lam JWY, Zhao ZJ, Tang BZ. Y-Shaped Pyrene-Based Aggregation-Induced Emission Blue Emitters for High-Performance OLED Devices. *Adv. Optical Mater.* 2022;2200917.
- [23] Merz J, Dietz M, Vonhausen Y, Wöber F, Friedrich A, Sieh D, Krummenacher I, Braunschweig H, Moos M, Holzapfel M, Lambert C, Marder TB. Synthesis, Photophysical and Electronic Properties of New Red-to-NIR Emitting Donor–Acceptor Pyrene Derivatives. *Chem. Eur. J.* 2020;26:438–453.
- [24] Yang J, Huang J, Sun N, Peng Q, Li Q, Ma D, Li Z. Twist versus Linkage Mode: Which

One is Better for the Construction of Blue Luminogens with AIE Properties? Chem. – Eur. J. 2015;21:6862–6868.

[25] Yang J, Li L, Yu Y, Ren Z, Peng Q, Ye S, Li Q, Li Z. Blue pyrene-based AIEgens: inhibited intermolecular π – π stacking through the introduction of substituents with controllable intramolecular conjugation, and high external quantum efficiencies up to 3.46% in non-doped OLEDs. Mater. Chem. Front. 2017;1:91–99.

[26] Yang J, Qin J, Ren Z, Peng Q, Xie G, Li Z. Pyrene-Based Blue AIEgen: Enhanced Hole Mobility and Good EL Performance in Solution-Processed OLEDs. Molecules 2017;22:2144.

[27] Liu Y, Shan T, Yao L, Bai Q, Guo Y, Li J, Han X, Li W, Wang Z, Yang B, Lu P, Ma Y. Isomers of Pyrene–Imidazole Compounds: Synthesis and Configuration Effect on Optical Properties. Org. Lett. 2015;17:6138–6141.

[28] Xie FL, Ran HJ, Duan XW, Han RJ, Sun HM, Hu JY. 1,3,5,9-Tetra(4-(1,2,2-triphenylvinyl)phenyl)pyrene (TTPE(1,3,5,9)Py): a prominent blue AIEgen for highly efficient nondoped pure-blue OLEDs. J. Mater. Chem. C. 2020;8:17450–17456.

[29] Feng X, Qi C, Feng HT, Zhao Z, Sung HHY, Williams ID, Kwok RTK, Lam JWY, Qin A, Tang BZ. Dual fluorescence of tetraphenylethylene-substituted pyrenes with aggregation-induced emission characteristics for white-light emission. Chem. Sci. 2018;9:5679–5687.

[30] Xie FL, Yang XL, Jin PC, Wang XT, Ran HJ, Zhang HL, Sun HM, Su SJ, Hu JY. Achieving Simultaneously Ultrahigh Brightness, Extremely Low Efficiency Roll-Off and Ultralong Lifetime of Blue Fluorescent OLEDs by Using Donor–Acceptor-Type 5,9-Diarylamine Functionalized Pyrenes. Adv. Optical Mater. 2023;11:2202490.

[31] Thomas KRJ, Maurya A, Nagar MR, Jou JH. Tuning hybridized local and charge transfer emission in pyrene derivatives by incorporating phenanthroimidazole to realize high exciton harvest in blue organic light-emitting diodes. Dyes Pigments 2023;210:111008.

[32] Wang CZ, Pang ZJ, Yu ZD, Zeng ZX, Zhao WX, Zhou ZY, Redshaw C, Yamato T. Short axially asymmetrically 1,3-disubstituted pyrene-based color-tunable emitters: Synthesis, characterization and optical properties. Tetrahedron 2021;78:131828.

[33] Wang CZ, Feng X, Kowser Z, Wu C, Akther T, Elsegood MRJ, Redshaw C, Yamato T. Pyrene-based color-tunable dipolar molecules: synthesis, characterization and optical properties. Dyes Pigments 2018;153:125–131.

- [34] Yu ZD, Dong XX, Cao JY, Zhao WX, Bi GH, Wang CZ, Zhang T, Rahman S, Georghiou PE, Lin JB, Yamato T. Substituent effects on the intermolecular interactions and emission behaviors in pyrene-based mechanochromic luminogens. *J. Mater. Chem. C* 2022;10:9310–9318.
- [35] Wang CZ, Ichiyanagi H, Sakaguchi K, Feng X, Elsegood MRJ, Redshaw C, Yamato T. Pyrene-Based Approach to Tune Emission Color from Blue to Yellow. *J. Org. Chem.* 2017;82:7176–7182.
- [36] Xie ZL, Chen CJ, Xu SD, Li J, Zhang Y, Liu SW, Xu JR, Chi ZG, White-light emission strategy of a single organic compound with aggregation-induced emission and delayed fluorescence properties. *Angew. Chem. Int. Ed.* 2015;54:7181–7184.
- [37] Kim MJ, AhnM, Wee KR. Facile intra- and intermolecular charge transfer control for efficient mechanofluorochromic material. *Mater. Adv.* 2021;2:5371–5380.
- [38] Wang XH, Wang LR, Mao XY, Wang QS, Mu ZF, An L, Zhang W, Feng X, Redshaw C, Cao CY, Qin AJ, Tang BZ. Pyrene-based aggregation-induced emission luminogens (AIEgens) with less colour migration for anti-counterfeiting applications. *J. Mater. Chem. C* 2021;9:12828–12838.
- [39] Zhao ZJ, Chen SM, Lam JWY, Wang ZM, Lu P, Mahtab F, Williams DL, Ma YG, Kwok HS, Tang BZ. Pyrene-substituted ethenes: aggregation-enhanced excimer emission and highly efficient electroluminescence. *J. Mater. Chem. A* 2011;21:7210–7216.
- [40] Wang C, Li Z. Molecular conformation and packing: their critical roles in the emission performance of mechanochromic fluorescence materials. *Mater. Chem. Front.* 2017;1:2174–2194.
- [41] Grimme S, Antony J, Ehrlich S, Krieg H. A consistent and accurate ab initio parametrization of density functional dispersion correction (DFT-D) for the 94 elements H-Pu. *J. Chem. Phys.* 2010;132:154104.
- [42] Liu J, Zhang Y, Zhang K, Fan J, Wang CK, Lin L. Bicolor switching mechanism of multifunctional light-emitting molecular material in solid phase. *Org. Electron.* 2019;71:212–219.
- [43] Rajamalli P, Senthilkumar N, Gandeepan P, Huang PY, Huang MJ, Wu CZR, Yang CY, Chiu MJ, Chu LK, Lin HW, Cheng CH. A New Molecular Design Based on Thermally Activated Delayed Fluorescence for Highly Efficient Organic Light Emitting Diodes. *J. Am.*

Chem. Soc. 2016;138:628–634.